Confined Alpha Distribution Measurements in a Deuterium-Tritium Tokamak Plasma

G. McKee,[1] R. Fonck,[1] B. Stratton,[2] R. Bell,[2] R. Budny,[2] C. Bush,[3] B. Grek,[2] D. Johnson,[2] H. Park,[2] A. Ramsey,[2] E. Synakowski,[2] and G. Taylor[2]

[1]*Department of Nuclear Engineering and Engineering Physics, University of Wisconsin, Madison, Wisconsin 53706*
[2]*Princeton Plasma Physics Laboratory, P.O. Box 451, Princeton, New Jersey 08543*
[3]*Oak Ridge National Laboratory, Oak Ridge, Tennessee 37830*

(Received 27 February 1995)

Fusion-produced alpha particles with energy ≤ 0.7 MeV have been spectroscopically observed in the core of a deuterium-tritium plasma in the TFTR tokamak at alpha densities of 3×10^{16} m^{-3}. During a sawtooth-free discharge, the measured energy spectra at $r/a = 0.3$ are in good agreement with those predicted on the basis of collisional transport. Time-resolved measurements during the alpha thermalization after alpha source turn-off show decay of the distribution function to lower energies consistent with the classical slowing-down time of 0.5 s.

PACS numbers: 52.55.Pi, 52.25.Rv, 52.55.Fa

Knowledge of the dynamics and confinement of alpha particles is crucial to the development of a deuterium-tritium (DT) tokamak fusion reactor. Alpha particles, born at an energy of 3.5 MeV, carry 20% of the energy released in the DT reaction. If effectively confined, the alpha power can maintain the plasma energy against radiative and thermal transport losses without the need for external heating sources and thus lead to thermonuclear ignition. In addition to the effects of slowing-down and collisionally driven cross-field transport, these alphas may be subject to anomalous losses due to phenomena such as MHD, sawteeth, and toroidal Alfvén eigenmodes [1–3]. While previous studies have concentrated on the behavior of fast plasma ions [4], the ongoing DT experiments on the Tokamak Fusion Test Reactor (TFTR) [5,6] provide the first opportunity to directly observe the behavior of the confined alpha particles in a reactor-grade fusing DT plasma.

This Letter reports the first absolutely calibrated measurement of nonthermal confined alpha particles in a DT tokamak plasma. The measurements were made with the alpha particle charge exchange recombination spectroscopy (α-CHERS) diagnostic, a visible spectroscopic diagnostic designed to observe the nonthermal confined alpha population during DT experiments on TFTR [7]. The alpha particles are observed by measuring spectral line emission resulting from charge exchange reactions between TFTR heating neutral beam particles and confined alpha particles. The charge exchange reaction rate for line emission resulting from the (T^0, α) or (D^0, α) reactions is significant only for squared relative velocities in the neighborhood of 30 keV/amu [8]. Thus, only the lower energy range of the slowing-down distribution ($E_a \leq 0.7$ MeV) is typically accessible for the 50–60 keV/amu beam energy available on TFTR. Deuterium rather than tritium beams are used for this diagnostic due to their higher velocity at a given energy and deeper beam penetration into the core of the plasma. Tritium was injected by beams not observed with α-CHERS, yielding a roughly 50-50 density ratio of deuterium and tritium in the plasma core.

The beam-sightline geometry is designed to yield a redshift of the nonthermal α signal, allowing it to be separated from the background thermal helium emission line. For the visible 4-3 He II ($\lambda_0 = 468.6$ nm) transition observed by α-CHERS, emission from 0 to 0.7 MeV alpha particles is Doppler shifted over an 8 nm spectral region.

The alpha signal is expected to be less than 1% of the bremsstrahlung intensity and is near the wings of the much brighter thermal He II line emitted from cool edge helium and neautral beam charge exchange reactions with core thermal helium. Extraction of the signal from this background requires excellent photon statistics, necessitating the high throughput, moderate resolution spectrometer, and low-noise, high-quantum-efficiency, high-dynamic-range detectors incorporated into the α-CHERS system [9]. Assuming that the measured signal is photon-noise dominated, the alpha signal is predicted to be observable with a signal-to-noise ratio of 5–10 in high power DT discharges on TFTR. Measurements are typically averaged over a 100–400 ms interval to improve the photon statistics. The ability to observe a nonthermal helium ion population via α-CHERS was experimentally demonstrated earlier by observation of ^{3}He ions at several hundred keV which were produced by ion cyclotron resonance frequency minority heating [10].

A DT experiment designed to allow for alpha detection with α-CHERS was performed on TFTR. The discharges were supershots similar to those described by Strachan *et al.* [6] and had $B_t = 5.1$ T, $I_p = 2.0$ MA, $R = 2.52$ m, and $a = 0.87$ m. Peak alpha densities $>1 \times 10^{17}$ m^{-3} were produced in these experiments, with a fusion power output of up to 6 MW. Observed lost alpha behavior was consistent with classical first-orbit loss expectations [11], and no evidence of collective alpha-driven

0031-9007/95/75(4)/649(4)$06.00

instabilities adversely affecting the alpha particle confinement was observed. The deuterium and tritium beams were injected into a deuterium target plasma and operated simultaneously from 2.8 to 4.1 s to maximize the fusion-produced alpha density and to yield a quasi-steady-state alpha density, while the deuterium beams were extended to 4.8 s to permit observation of the alphas as they thermalized after tritium beam turn-off, as shown in Fig. 1. The neutron/alpha production rate [Fig. 1(b)] for the discharge under study peaks at $1.5 \times 10^{18} n/s$ at 3.3 s rolls off slowly until the tritium beams turn off, and then decays rapidly. Also shown in Fig. 1 are the line-averaged electron density and stored energy for a typical shot during this experiment. In this experiment a total of four shots were available where the α-CHERS measurements in the core region can be expected to provide a reasonable signal-to-noise ratio. Of these four, only one was free of strong sawteeth in the post-T^0 beam phase, and α-CHERS provided measurements at $r/a = 0.3$ for this case. The results for this sawtooth-free case are discussed in detail here to evaluate the behavior of fusion-produced alphas in a nonsawtoothing discharge, where classical slowing down and transport might be expected.

The period 4.3–4.8 s is of primary interest for this experiment since substantial numbers of alphas have slowed to observable energies by this time; the analysis is simplified because radiation effects on the optical fibers are minimized [12,13], and the thermalization process can be observed as a result of the 0.5 s alpha slowing-down time. Techniques to compensate for fluorescence and transmission changes of the optical fibers due to radiation during the DT phase of the discharge are presently under development, and this Letter discusses data only from the period 4.3–4.8 s.

Several low-intensity impurity lines emitted by low charge states of carbon exist in the spectral region of interest, 468–480 nm, as seen in the typical α-CHERS spectrum shown in Fig. 2. These impurity lines are removed from the spectrum by fitting them with a Gaussian line shape convolved with the measured instrumental line profile on a local linear background and by subtracting the fitted model from the spectrum. The noise level of the residual (data minus fit) has rms values equal to photon statistical noise, indicating that the line removal process does not add systematic noise to the data.

Each DT shot performed in this experiment had a corresponding DD shot with similar plasma parameters (n_e, T_e, and Z_{eff}), and thus a similar bremsstrahlung intensity, varying by less than 5% from the DT shot in question at all time points of interest. Changes in the wavelength dependence of the bremsstrahlung spectrum due to the observed minor differences between the DD and DT shots were calcualted and found to be insignificant. Following subtraction of the impurity lines from each data set, the resulting spectrum consists of a pure bremsstrahlung spectrum, thermal helium line, and fast alpha signal (DT shot only). For $E_\alpha > 0.7$ MeV the fast alpha signal is negligible due to the rapidly falling line-excitation cross section, and thus no observable signal is expected [14]. The DD and DT spectra are normalized to each other in a spectral range corresponding

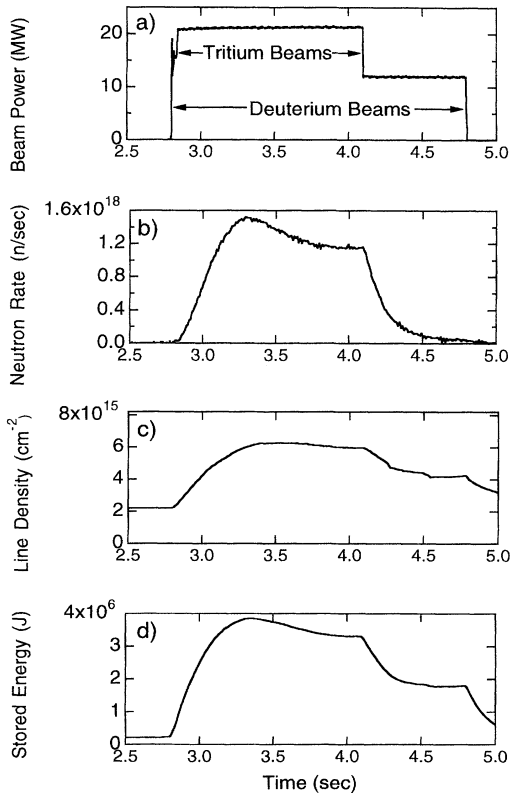

FIG. 1. Time evolution of (a) neutral beam power, (b) neutron rate, (c) electron line density, and (d) stored energy.

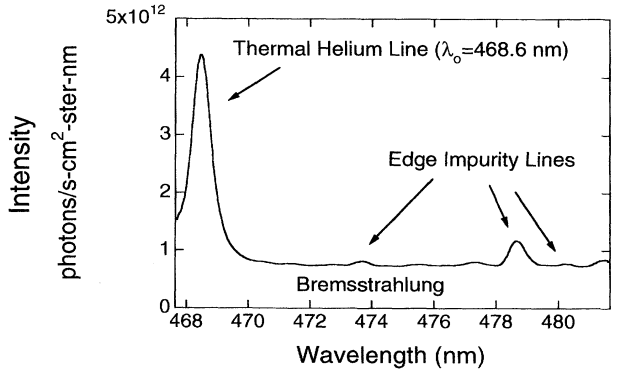

FIG. 2. α-CHERS spectrum from a DT shot showing thermal helium line, bremsstrahlung continuum, and edge impurity lines. The intensity of the alpha feature is approximately 1% of the bremsstrahlung and thus cannot be observed on this scale.

to alpha energies of 0.75–1.05 MeV, where the signal is bremsstrahlung only.

This normalization allows for an accurate subtraction of the data sets to yield the nonthermal alpha signal as shown in Fig. 3 for $r/a = 0.3$. The data are binned together in the spectral (energy) direction (0.8 nm per data point) to improve the signal-to-noise ratio. The alpha signal is broad and varies smoothly across the spectrum so the resulting energy resolution of 30–90 keV is more than adequate to compare with predicted signals. The signal intensity is plotted as a function of energy along the spectrometer line of sight, essentially $E_{\|}$ because of the viewing geometry. The error bars correspond to photon statistics associated with time averaging, spectral binning, and shot-to-shot subtraction. The data have been averaged over the 400 ms interval 4.3–4.7 s to improve the signal-to-noise ratio. The signal shown in Fig. 3 is an absolute radiance measurement; α-CHERS was absolutely calibrated using an integrating sphere light source and cross-calibrated with an independent measurement of the bremsstrahlung intensity from the HAIFA diagnostic [15] to account for transmission of the optical fibers and spatial variations in the light collecting optics.

In Fig. 3 the measured signal at $r/a = 0.3$ is compared to a predicted signal based on the alpha energy distribution calculated by the TRANSP kinetic analysis code [16]. TRANSP calculates the alpha distribution in space, time, energy, and pitch angle from the measured neutron rate and profile, electron and ion densities, and temperatures using a Monte Carlo method incorporating banana orbit width, finite gyroradius effects, and collisionally induced slowing down and transport arising from coupling to thermal species.

The predicted α-CHERS spectrum is calculated from the TRANSP alpha distribution using spectral modeling codes which include the neutral beam-viewing sightline geometry, beam parameters (energy, density, and physical dimensions), and energy-dependent, charge-exchange cross sections [14]. The predicted spectrum includes contributions from three sources: neutral beam charge exchange recombination with alphas, charge exchange between fast alphas, and beam-generated halo neutral particles, and electron and ion impact excitation of alpha plume ions created along the beam trajectory [17]. The halo neutrals are thermal neutrals that arise from beam-thermal ion charge exchange reactions along the beam trajectory, while the fast He^{+1} plume ions originate from charge exchange reactions between alphas and beam particles.

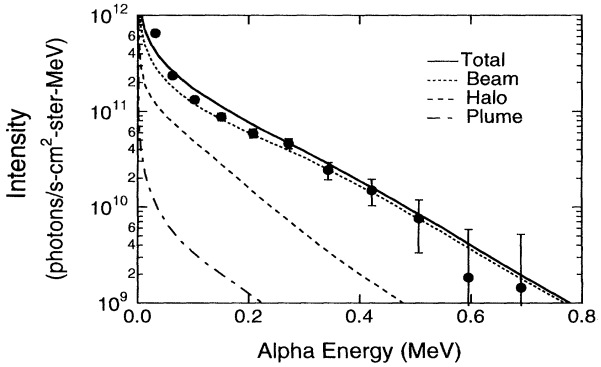

FIG. 3. Fast alpha signal (●) measured at $t = 4.3$–4.7 s at $r/a = 0.3$ and spectrum calculated from TRANSP distribution (—) at $t = 4.50$ s. Contributions from neutral beam charge exchange reactions, halo neutral reactions, and the ion plume are shown separately.

Since the nonthermal alphas have speeds equal to or greater than those of the beam and halo neutrals, the models include the appropriate velocity-space integrals to obtain the excitation rates for a given alpha speed along the line of sight. Likewise, the ion plume model accounts for the anisotropic velocity distribution function of the He^+ ions produced by alpha-neutral charge exchange. As shown in Fig. 3, the beam-alpha reactions contribute the bulk of the signal, with the halo neutrals contributing up to a third of the signal at low energies (<300 keV), but dropping rapidly at higher energies due to the falloff in charge-exchange cross section with relative energy. The ion plume signal is seen to contribute little to the overall signal because the sharp decrease in alpha density with minor radius, with alphas at larger radii being the primary source of plume ions for the given sightline geometry.

The slowing-down alpha signal measured with α-CHERS agrees well in absolute magnitude and spectral shape with the model spectrum, indicating that the alpha energy distribution is close to that predicted by collisional slowing down and transport and that no significant anomalous losses of the fast alphas occur in these discharges. The total alpha density at $r/a = 0.3$ predicted by TRANSP is 3.3×10^{16} m^{-3}. Note that the measured and predicted spectra in this and following figures are not normalized to each other, but rather are independently arrived at with no adjustable parameters in either the data or the model values. The absolute intensity agreement obtained is as good as could be expected given that systematic uncertainties in the spectral radiance calibration, atomic cross sections, and the Monte Carlo calculation of the alpha distribution in TRANSP can combine to yield a roughly 30% uncertainty in the comparison between model and measurement.

The signal-to-noise ratio of this data set is sufficient to allow examination of smaller time intervals of 100 ms to study the evolution of the thermalization of the alpha distribution. 100 ms time resolution is suitable for this measurement since the source of alphas is turned off at 4.1 s, and the alphas have a slowing-down time of about 0.5 s. As a result, the alpha population should undergo substantial thermalization during the time period under observation. The time evolution of the measured and predicted signals is shown in Fig. 4. Both the α-CHERS

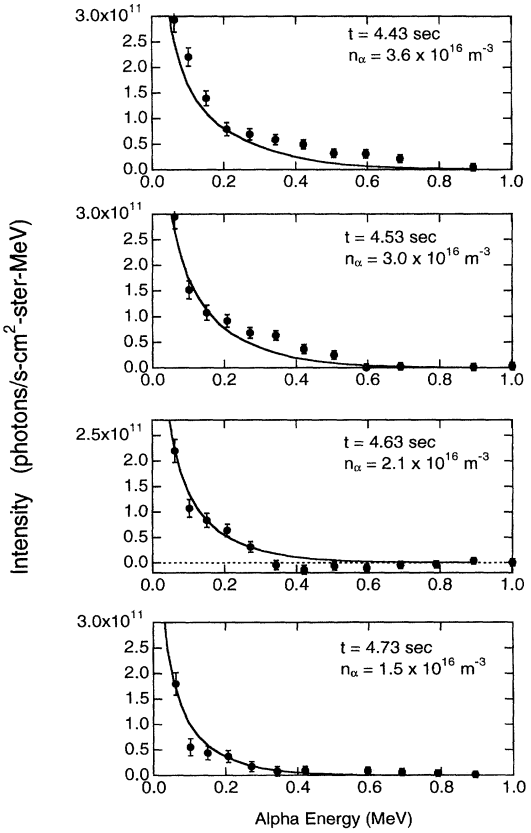

FIG. 4. Time evolution of fast alpha distribution at four time points during thermalization process, showing decay of the distribution to lower energies after source turn-off at 4.1 s; 100 ms integration time at $r/a = 0.3$. ● indicates α-CHERS measurement and — indicates the spectrum calculated from the TRANSP α distribution.

data and the model spectra exhibit a decay of the alpha distribution to lower energies with time that is consistent with classical slowing down.

As mentioned earlier, the data shown here are from a discharge in which no sawteeth occurred. Other shots in this experiment with sawteeth in the post T^0 beam phase typically show a reduced intensity of the fast alpha signal, suggesting that sawteeth influence the alpha population at the observation point, which is inside the sawtooth inversion radius. However, relatively poor signal-to-noise ratio and irreproducible sawtooth crash times prevent any conclusion other than this qualitative observation to be drawn from these first experiments on the effects of sawteeth. Future experiments are proposed to address in detail the effect of sawtooth crashes on the fast alpha population.

In conclusion, the lower energy alpha distribution produced in a TFTR DT plasma has been observed by the α-CHERS diagnostic in a sawtooth-free discharge. The intensities of the resulting signals are in good agreement with the expected signal intensities from the calculated alpha distribution, indicating that neoclassical predictions of the confinement and behavior of the alpha distribution are consistent with observations. This is also consistent with measurements from the lost alpha detectors [11], which indicate that the losses are dominated by first-orbit losses of a few percent of the alpha population and that no anomalous losses due to collective alpha behavior or MHD are occurring.

The authors would like to thank R. Ashley, D. Cylinder, and M. Vocaturo for their assistance with the diagnostic hardware, and T. Gibney, P. Roney, N. Schechtman, and H. Towner for software support. J. Strachan provided invaluable assistance with optimizing the performance of TFTR. This research was performed under appointment to the Magnetic Fusion Energy Technology Fellowship program administered by the Oak Ridge Institute for Science and Education for the U.S. Department of Energy and supported by DOE Contract No. DE-AC02-76CH03073 and Grant No. DE-FG02-89-ER53296.

[1] C. Z. Cheng, Phys. Fluids B **3**, 2463 (1991).
[2] C. T. Hsu and D. J. Sigmar, Phys. Fluids B **4**, 1492 (1992).
[3] D. J. Sigmar, C. T. Hsu, R. White, and C. Z. Cheng, Phys. Fluids B **4**, 1506 (1992).
[4] W. W. Heidbrink and G. J. Sadler, Nucl. Fusion **34**, 535 (1994).
[5] R. J. Hawryluk *et al.*, Phys. Rev. Lett. **72**, 3530 (1994).
[6] J. D. Strachan *et al.*, Phys. Rev. Lett. **72**, 3526 (1994).
[7] G. R. McKee *et al.*, Rev. Sci. Instrum. **66**, 643 (1995).
[8] M. G. von Hellermann *et al.*, Plasma Phys. Controlled Fusion **33**, 1805 (1991).
[9] T. A. Thorson, G. McKee, R. J. Fonck, and B. Stratton, Rev. Sci. Instrum. **63**, 5182 (1992).
[10] B. C. Stratton *et al.*, Nucl. Fusion **34**, 734 (1994).
[11] S. J. Zweben, Princeton Plasma Physics Laboratory Report No. PPPL-3045 (to be published).
[12] A. T. Ramsey, Rev. Sci. Instrum. **66**, 871 (1995).
[13] A. T. Ramsey and K. W. Hill, Rev. Sci. Instrum. **63**, 4735 (1992).
[14] B. C. Stratton, R. J. Fonck, G. McKee, and T. Thorson, Rev. Sci. Instrum. **63**, 5179 (1992).
[15] A. T. Ramsey and S. L. Turner, Rev. Sci. Instrum. **58**, 1211 (1987).
[16] R. V. Budney *et al.*, Nucl. Fusion **34**, 1247 (1994).
[17] R. J. Fonck, D. S. Darrow, and K. P. Jaehnig, Phys. Rev. A **29**, 3288 (1984).